Comparison between constant feedback and limiter controllers

C. T. Zhou[1,*] and M. Y. Yu[2]
[1]*DSO National Laboratories, 20 Science Park Drive, Singapore 118230*
[2]*Institut für Theoretische Physik I, Ruhr-Universität Bochum, D-44780 Bochum, Germany*
(Received 9 February 2004; revised manuscript received 12 October 2004; published 4 January 2005)

Using symbolic dynamics of the one-dimensional unimodal map, the chaos stabilization mechanics of the feedback and limiter control schemes are considered. For feedback control, it is found that the control strength can be efficiently obtained from the superstable parameter of the embedded periodic orbits, and the scaling of the control-space period-doubling bifurcation cascade still obeys the Feigenbaum law. For Sarkovskii orbits, the scaling is also consistent with that of the original chaotic system. For limiter control, a single critical point in the unimodal map is extended to a superstable periodic window and a simple approach for determining the value of the control plateau is found. The scaling in the control space of the period-doubling bifurcation cascade is indeed superexponential. A different scaling for the fine structure of the Sarkovskii sequence is also found. Simple one-dimensional unimodal maps can also be used to generate maximum-length shift-register sequences.

DOI: 10.1103/PhysRevE.71.016204 PACS number(s): 05.45.Gg, 05.45.Ra, 05.45.Vx

I. INTRODUCTION

Most proposals for applying chaos to spread spectrum communication are based on the assumption that a chaotic system can generate an ideal scrambling/spreading code consisting of an *infinite* sequence of random codes, an unrealistic task for finite digital hardware. Thus, in practice periodic pseudorandom (PN) sequences are used instead [1]. The most widely used binary PN code sequences are the maximum-length shift-register (or *m*) sequences, Gold sequences, and Kasami sequences [1–3]. For applications in spread spectrum communication, ranging, and analog-digital conversion, etc., other binary sequences, especially nonlinear ones, may be suitable. For example, existing works [4–6] show that truncated and quantized chaotic sequences allow performances that are superior to the classical ones.

On the other hand, by definition chaos consists of an infinite number of unstable periodic orbits (UPOs). In principle, stable or unstable periodic orbits of arbitrary length in a given chaotic system can be determined to any desired accuracy, so that a tailored set of such periodic sequences can be very useful [7–10]. In using UPO binary sequences for digital communication, it is necessary to find suitable control parameters for the selected chaotic system in order to optimize the digital machines generating the codes. A direct strategy is to apply the known stabilization techniques of chaos to control the long periodic orbits, so that the desired PN sequence is robustly generated.

At present the most important still open task is to stabilize the desired orbits at high periodicity. In general, orbits become more difficult to stabilize as the periodicity increases. Usually the use of special control techniques is required [11,12]. There are two basic methods to control chaos. The first is to stabilize the unstable periodic orbits embedded within a chaotic attractor, using for example the Ott, Grebogi, and Yorke approach [13]. The second is to convert the chaotic behavior into periodic behavior, using for example the constant feedback (CF) [14] or limiter control [15–20]. Because of its simplicity, the CF method has been applied extensively to one [21–23] and higher-dimensional maps [24], spatiotemporal dynamics [25], hyperchaos [26], as well as continuous-time systems [27]. More recently, introduction of limiter control gave us a practical way to control high-speed systems [15–18]. To apply these approaches to our problem, one first needs to estimate the control parameters such that chaos is stabilized or converted into periodic orbits.

Here we present a simple parameter estimating scheme for both the CF and limiter controllers. Although substantial knowledge already exists in this area [21,22,28], some unclear points are still unsolved, such as determining the control parameters of arbitrary periodic orbits and comparing the ability of both controllers to stabilize high-periodicity orbits. We are especially interested in a periodic PN sequence generator based on simple chaotic systems. A basic ingredient of our method is to apply symbolic dynamics of a one-dimensional (1D) unimodal map to the control system. By employing the standard word-lifting technique of symbolic dynamics [29,30], we show that the strength of the control system can be numerically estimated. For specific maps, such as the digital tent map, even analytical results can be found. Once the appropriate control parameters are estimated for a given periodic sequence, one can employ the corresponding chaotic system to generate the desired binary sequence robustly with zero waiting time. With such an implementation, the controlled chaotic system as a finite-state machine can be used in spread spectrum communication and many other digital applications.

The paper is organized as follows. In Sec. II, we briefly review the basic properties of the CF and limiter controllers, and apply symbolic dynamics of 1D unimodal maps to these two methods. Section III deals with applying the word-lifting technique in choosing the appropriate control parameters. We

*Present address: Institute of Applied Physics and Computational Mathematics, P. O. Box 8009, Beijing 100088, People's Republic of China.

also investigate how to generate m sequences by using 1D unimodal maps with the limiter control technique. In Sec. IV, the scaling of period-doubling systems and Sarkovskii sequences for both control methods is analyzed numerically and analytically. For the digital tent map with the limiter control approach, the parameter values corresponding to Sarkovskii sequences are analytically given. The main results are summarized and discussed in the final section.

II. CONTROLLING CHAOS BY CF AND LIMITER SCHEMES

The basic mechanism for controlling chaos can be understood by analyzing the 1D map $x_{n+1}=f(x_n,a)$, where x_n is the system state and a is the system parameter. In this study, we consider control of systems whose dynamics can be described by 1D unimodal maps, especially the logistic and tent maps. In the next subsections we shall apply symbolic dynamics techniques to these two 1D maps.

A. Constant feedback controller

In this method, a CF is added at each iteration to the right-hand side of the function $f(x_n,a)$. It follows that

$$x_{n+1} = f(x_n,a) + \gamma, \tag{1}$$

where $\gamma \in \Re$ indicates the strength of the feedback control. Parthasarathy and Sinha [14] first applied this method to the logistic and exponential maps for specific parameter values and initial conditions. They found convergence to fixed points and periodic points. Gueron [21] presented an analytical description of the algorithm, and proved that a γ exists such that the system (1) converges to a fixed point if f is a unimodal function.

Another interpretation of the CF method (1) is to assume that the variable x_n can be superimposed at each iteration by a constant pulse. The corresponding equation is then [23,24]

$$x_{n+1} = f(x_n + \gamma, a), \tag{2}$$

so that the map is controlled by changing x_n in such a way that an appropriate feedback is applied in the form of pulses.

B. Limiter controller

Recently Corron and co-workers [15,16] introduced a different control approach, namely, control by simple limiters, such that control is realized when a certain variable exceeds a threshold. Their approach was successfully tested for different conditions, and a period-34 UPO in a low-frequency circuit was successfully demonstrated. Stoop and Wagner [19] analyzed simple limiter controllers, and found that control is limited by superexponential scaling in the control space [20]. Here we shall provide a systematic theory. For 1D discrete maps, the control scheme is implemented by [15–20]

$$x_{n+1} = \begin{cases} f(x_n,a) & \text{if } f(x_n,a) < \gamma, \\ \gamma & \text{if } f(x_n,a) \geqslant \gamma, \end{cases} \tag{3}$$

where γ is the limiter parameter. As will be shown below, the parameter γ is directly related to the height of the limiter control. We shall therefore denote $h \equiv \gamma$ for this control scheme.

C. Symbolic dynamics of control systems

We are interested in the unimodal function $f(x)$. It is obvious that Eqs. (1) and (2) are still unimodal maps since the strength γ of the feedback only realizes a translation of a function vector in the (x,f) plane. For example, a 1D map is translated up or down the vertical axis if Eq. (1) is used, and it is translated left or right of the x axis if Eq. (2) is used. For the system (3), the problem is somewhat difficult, since a single critical point (x_c) in the original system now becomes a finite window $[x_c-\epsilon_l, x_c+\epsilon_r]$, where ϵ_l and ϵ_r denote the left and right boundary values of the control window. Associated with each superstable periodic orbit (SPO) of period k is a window in which orbits of period k are stable. If we treat this control window as a single critical point x_c, we could still say that the limiter control system (3) is a unimodal map. However, this finite superstable window leads to disappearance of the chaos, while the periodic orbits remain. Moreover, any orbit of the system (3) is a periodic orbit as long as $h \neq f(x_c)$. To generate a desired orbit, one has to calculate the corresponding parameter value h.

It is convenient to rewrite Eqs. (1)–(3) in the form

$$x_{n+1} = f(x_n,a,\gamma), \tag{4}$$

such that the time series $\{x_n, n=0,1,2,\ldots\}$ of this equation corresponds to an orbit of the map with initial condition x_0. The symbolic description of a given x_n is defined as $s=1$ or R if $x_n > x_c$ and $s=0$ or L if $x < x_c$. The symbol string $S = s_0 s_1 s_2 \cdots$ with $s_n \in \{0,1\}$ or $s_n \in \{R,L\}$ is the forward itinerary of the initial point x_0. A periodic orbit of length n is a real solution of $f^{(n)}(x) = f(f(\cdots f(x)\cdots)) = x$. Obviously the latter has 2^n solutions in the complex space, and there will be 2^n or less period-n orbits for the map. A periodic orbit is stable if $|df^{(n)}(x)/dx| = |f'(x)f'(f(x))\cdots f'(f(f(\cdots f(x)\cdots)))|_{x_0} < 1$, and superstable if the orbit intersects the critical point x_c, that is, $df^{(n)}(x)/dx|_{x_c} = 0$. The symbol string obtained by $x_0 = \tilde{x}_c$ is of special interest and is called the superstable period orbit. Here $\tilde{x}_c \equiv x_c$ for the CF control, and $\tilde{x}_c \in [-\epsilon_l + x_c, x_c + \epsilon_r]$ for the limiter control.

For a periodic sequence, $(RL^{n_1}R^{n_2}\cdots QC_s)^\infty$, where $Q=R$ or L, and C_s is associated with the critical point $\tilde{x}_c$. The corresponding equation for this superstable periodic sequence is

$$f_R^{-1}(f_L^{-1,n_1}(f_R^{-1,n_2}(\cdots(f_Q^{-1}(\tilde{x}_c,a,\gamma))\cdots))) = f(\tilde{x}_c,a,\gamma), \tag{5}$$

where

$$f_Q^{-1,n} = \underbrace{f_Q^{-1}(f_Q^{-1}(\cdots))}_{n},$$

and f_R^{-1} and f_L^{-1} are the inverse functions of f. For $\gamma=0$, it is in general easy to obtain from Eq. (5) an iterative solution of the parameter a for a SPO [29,30]. Furthermore, the control parameter γ can also be estimated if the system parameter a is given.

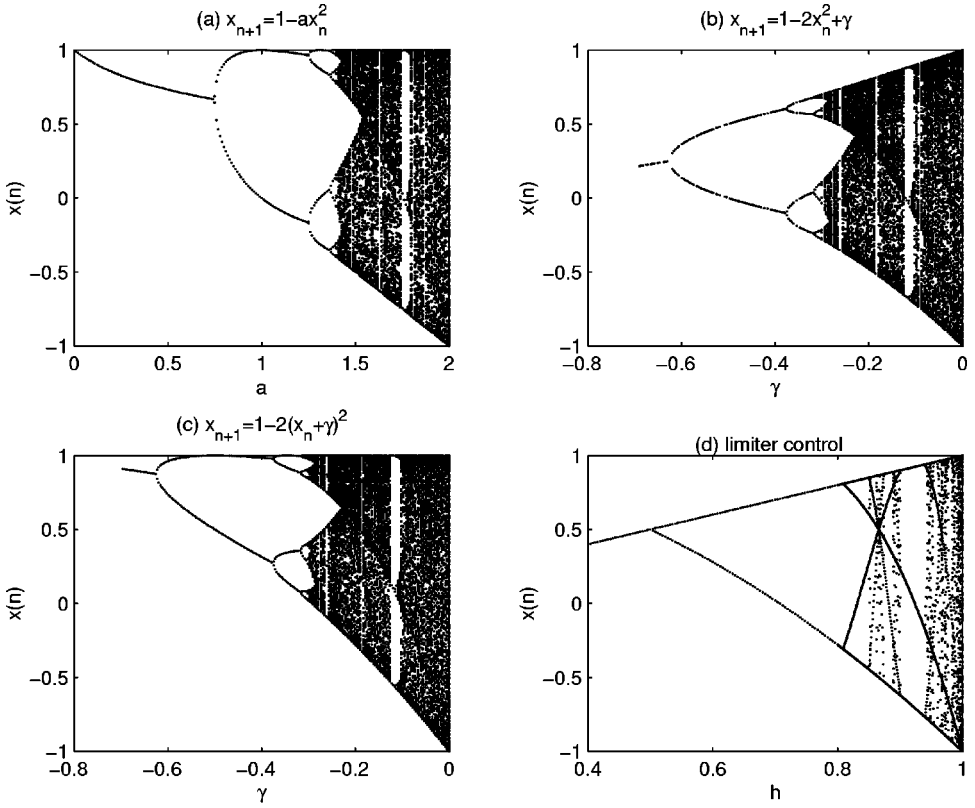

FIG. 1. Bifurcation behavior of the logistic map and the corresponding control systems. (a) Logistic map, (b) constant feedback control (6), (c) constant feedback control (7), and (d) limiter control (9).

III. CHOICE OF CONTROL PARAMETERS

In general, orbits become more difficult to stabilize as the periodicity increases. Existing studies usually invoke rather complicated methods, such as the evolutionary algorithm [22], or network training based on genetic algorithm evolution [28], to find the best control parameter value such that the controlled orbit is closest to the desired one. In the following, we shall show that the control strength in Eqs. (1)–(3) can easily be calculated using symbolic dynamics for an arbitrarily long periodic orbit.

A. Constant feedback control

We consider the logistic map $f(x,a)=1-ax^2$. Eqs. (1) and (2) then become

$$x_{n+1} = 1 - ax_n^2 + \gamma \tag{6}$$

and

$$x_{n+1} = 1 - a(x_n + \gamma)^2, \tag{7}$$

where again the control parameters are a (bifurcation parameter) and γ (strength of feedback). When $\gamma=0$, this discrete system exhibits standard period doubling and onset of chaos as a is increased. Figure 1(a) shows a typical bifurcation diagram of the logistic map. The period-doubling bifurcation cascade here obeys the Feigenbaum scaling law [31]: $a_\infty - a_n \sim \delta^{-n}$, with $\delta=4.669\,201\,609\,103\ldots$.

Figures 1(b) and 1(c) show the behavior of the two feedback control schemes as given by Eqs. (6) and (7) for $a=2$, corresponding to a system with fully developed chaos. Period-doubling bifurcations can clearly be observed as γ is increased. Chaos appears when $\gamma \to \gamma_\infty$. The feedback strength γ in Eqs. (6) and (7) therefore behaves like the bifurcation parameter a of the original logistic map.

We now consider the operation of the two control schemes. For illustration, we use a superstable periodic sequence $RLRC_s$. For the original logistic map, the value of a^s for this SPO is easily calculated from Eq. (5), which can be written explicitly in iterative form as [30] $a_{n+1} = \sqrt{a_n + \sqrt{a_n - \sqrt{a_n}}}$. The iteration converges rapidly for any reasonable initial value $a_0 \in (0,2]$, and yields $a^s = \lim_{n\to\infty} a_n \approx 1.310\,702\,641\,336\,8332$. The procedure in forming this SPO is shown in Fig. 2(a).

For the CF control (6), using Eq. (5) for the SPO $RLRC_s$, one easily obtains

$$\gamma = a^s/a - 1, \tag{8}$$

so that to determine the control strength γ, we should first compute the corresponding superstable parameter a^s from the original chaotic system $f(x,a,0)$. Accordingly, we obtain for the SPO $RLRC_s$ the value

$$\gamma \approx 1.310\,702\,641\,336\,833\,2/2 - 1$$
$$\approx -0.344\,648\,679\,331\,583\,4.$$

Figure 2(b) shows the control procedure of the CF scheme. Clearly, the control map function $f(x,a,\gamma)$ is a downward translated version of the original chaotic system $f(x,a,0)$. We note that the expression (8) can also be obtained by transforming the control system (6) into the standard form of the logistic map: $x'_{n+1}=1-a'x'^2_n$ with $a'=a(1+\gamma)$ and $x'=x/(1+\gamma)$. If the parameter a' is associated with a SPO, we

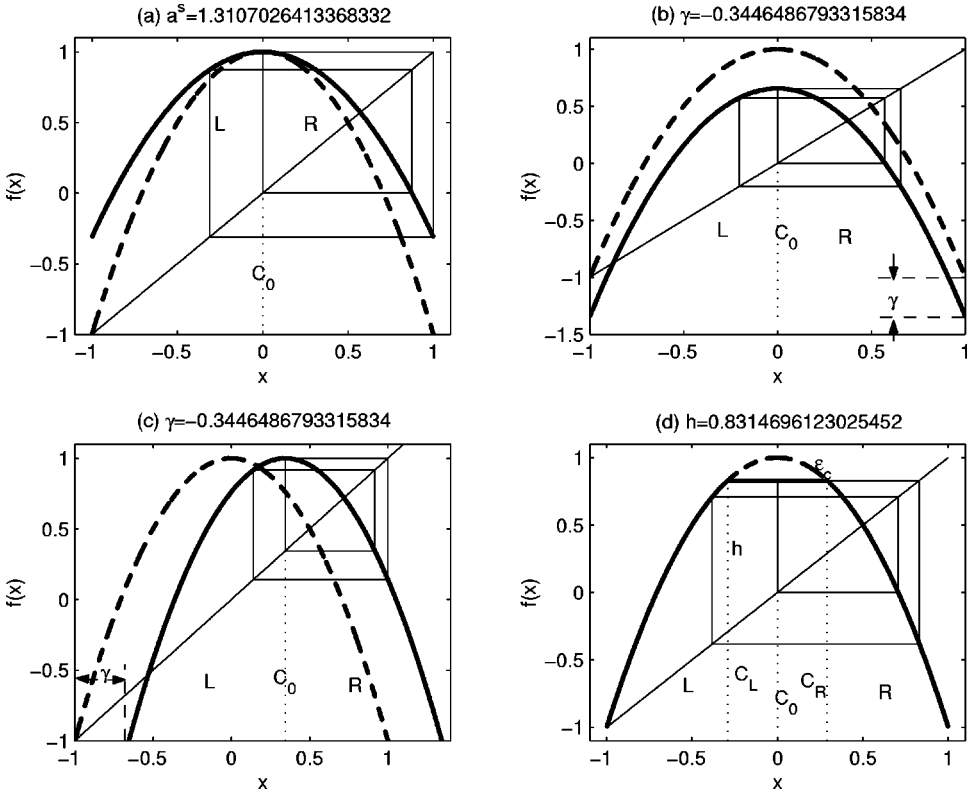

FIG. 2. Geometrical interpretation of the mechanism of control of chaos in the logistic map. The dashed line corresponds to fully developed chaos $a=2$. (a) Superstable orbit $RLRC_s$, (b) stabilization procedure using constant feedback control (6), (c) stabilization procedure using constant feedback control (7), and (d) stabilization procedure using limiter control (9).

readily get the expression (8). This linear transformation implies that both the logistic map and the corresponding CF control system (6) are of equivalent topology. When γ continuously varies from some negative value to zero, all the SPOs in the original logistic map would appear, provided that a proper initial condition is used. The analysis here provides an explicit mapping of the controlled system to the uncontrolled one at a different parameter setting. This relationship is of interest since it implies that the search for good parameter values amounts to identifying the parameter values for the periodic windows in the quadratic map.

The control system (7) is stabilized by applying appropriate pulses γ to the system variable. Mathematically, the map function in Eq. (7) is only a left- or right-shifted version of the original logistic map illustrated in Fig. 2(c). Its symbolic description is thus consistent with that of the controlled logistic map Eq. (6). Setting $x_n'=x_n+\gamma$, we can transform Eq. (7) into $x_{n+1}'=1-ax_n'^2+\gamma$, which is equivalent to Eq. (6). Thus, for an arbitrarily given admissible sequence, Eqs. (6) and (7) give the same control strength $\gamma=a^s/a-1$.

In order to stabilize the uncontrolled logistic map on the nearest $(k+1)$-periodic SPO of the controlled logistic map, we can add one more symbol C_s to the sequence by taking into account a k-periodic UPO sequence of the latter. For this SPO, the strength of the feedback control can be numerically determined by using Eq. (8). For example, for a period-5 UPO *RLLRR*, the corresponding period-6 SPO is $RLLRRC_s$. The stabilization procedure is shown in Fig. 3(a), where $\gamma \approx 0.046\,359\,954\,467\,349$. Using this control parameter and the initial condition $x_0=0$ in Eq. (6), we obtain (recall that $a=2$) a stable periodic orbit, as shown in Fig. 3(b). Clearly, the transition time to form this periodic-6 SPO is zero, which means that the corresponding binary sequence 10011 generated via the CF control, as given in Fig. 3(c), is robust and has zero waiting time.

B. Limiter control: The logistic map

Using Eq. (3) for the logistic map, one gets

$$x_{n+1}=\begin{cases}1-ax_n^2 & \text{if } x_{n+1}<h,\\ h & \text{if } x_{n+1}\geqslant h,\end{cases} \tag{9}$$

and the corresponding period-doubling bifurcation cascade is shown in Fig. 1(d). We see that the bifurcation cascade clearly differs in scaling from the Feigenbaum cascade, and there is no chaos even beyond h_∞.

The stabilization mechanisms in the feedback (6) and limiter (9) control schemes are quite different. As shown in Fig. 2(d), the main strategy in the limiter control is to convert the location of the original unstable periodic orbits into the controller threshold of the controlled system, leading to the appearance of a finite superstable window in the new system. For the logistic map, the superstable window is $[-\epsilon_c+x_c,\epsilon_c+x_c]$ with $x_c=0$, and a stable periodic trajectory must eventually land on the plateau $h=1-a\epsilon_c^2$. A periodic orbit of length k corresponds to a real solution of $f^{(k)}(x)=f(f(\cdots f(x_0,a,h)\cdots))=h$. For an admissible symbolic sequence at fixed x_0 and a, we can also estimate the limiter parameter h from Eq. (5).

For the control system (9), we define the symbol rule

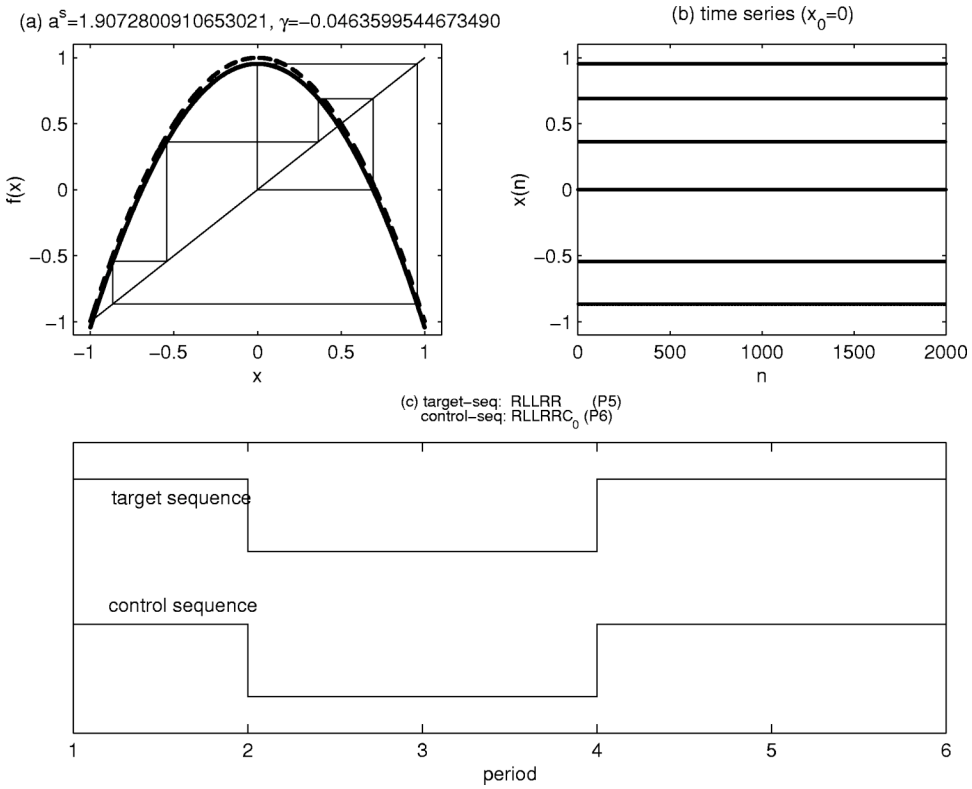

FIG. 3. The stabilization procedure of the target *RLLRR* using constant feedback control (6). The dashed line still corresponds to fully developed chaos $a=2$. (a) Geometrical representation, (b) time series, and (c) the binary representation.

$$s=\begin{cases} R & \text{if } x_n > \epsilon_c, \\ C_R & \text{if } 0 < x_n \leqslant \epsilon_c, \\ C_0 & \text{if } x_n \equiv 0, \\ C_L & \text{if } -\epsilon_c \leqslant x_n < 0, \\ L & \text{if } x_n < -\epsilon_c, \end{cases} \tag{10}$$

and set $f_{R,L}^{-1}=(+,-)\sqrt{(1-x_0)/a}$. Note that here three symbols (C_R, C_0, and C_L) are needed to denote C_s. The control parameter can then be calculated from

$$\epsilon_c=\sqrt{\frac{1}{a}\left(1-\frac{1}{a}g(a,x_0)\right)}, \tag{11}$$

where

$$g(a,x_0)=\sqrt{a+\sqrt{a\cdots\pm\sqrt{a(1-x_0)}}}, \tag{12}$$

and x_0 is defined by

$$x_0=\begin{cases} -\epsilon_c & \text{if } C_s=C_L, \\ 0 & \text{if } C_s=C_0, \\ \epsilon_c & \text{if } C_s=C_R, \end{cases} \tag{13}$$

so that for the orbit $RLRC_0$ shown in Fig. 2(d), we easily get $\epsilon_c \approx 0.290\,284\,677\,254\,462\,4$ and $h=1-2\epsilon_c^2 \approx 0.831\,469\,612\,302\,545\,2$.

To demonstrate the generation of UPO binary sequences, we consider the following three cases. A period-5 UPO *RLLRR* can be implemented by using $RLLRRC_0$, $RLLRRC_R$, and $RLLRRC_L$ [32], yielding $h \approx 0.970\,031\,253\,194\,544\,0$, 0.969 077 286 229 078 0, and 0.970 941 817 426 052 0, respectively. The stabilization procedure is shown in Fig. 4.

Unlike the CF method, where a unique control strength γ exists for a given periodic orbit, many (perhaps infinite) control values are possible in the limiter controller for the same SPO. This is because x_0 in Eqs. (11) and (12) can be continuously taken from the window $[-\epsilon_c, \epsilon_c]$. As will be shown in the following discussion on the digital tent map, the parameter x_0 determines the optimal configuration of the digital binary sequence generator.

C. Limiter control: The digital tent map

A controlled digital tent map is very useful for generating a long PN sequence. For example, consider the digital tent map [33], defined as

$$x_{n+1}=\begin{cases} 2x_n & \text{if } 0 \leqslant x_{n+1} < h/2, \\ h & \text{if } h/2 \leqslant x_{n+1} \leqslant B-h/2, \\ 2(B-x_n) & \text{if } B-h/2 < x_{n+1} \leqslant B, \end{cases} \tag{14}$$

where the state variable x_n and the base B are integers. We also define a symbol rule

$$s=\begin{cases} R & \text{if } B-h/2 < x_n \leqslant B, \\ C_R & \text{if } B/2 < x_n \leqslant B-h/2, \\ C_0 & \text{if } x_n = B/2, \\ C_L & \text{if } h/2 \leqslant x_n < B/2, \\ L & \text{if } 0 \leqslant x_n < h/2, \end{cases} \tag{15}$$

and set $f_R^{-1}=B-x_0/2$ and $f_L^{-1}=x_0/2$. For the digital tent map, Eq. (5) can thus be expressed explicitly as

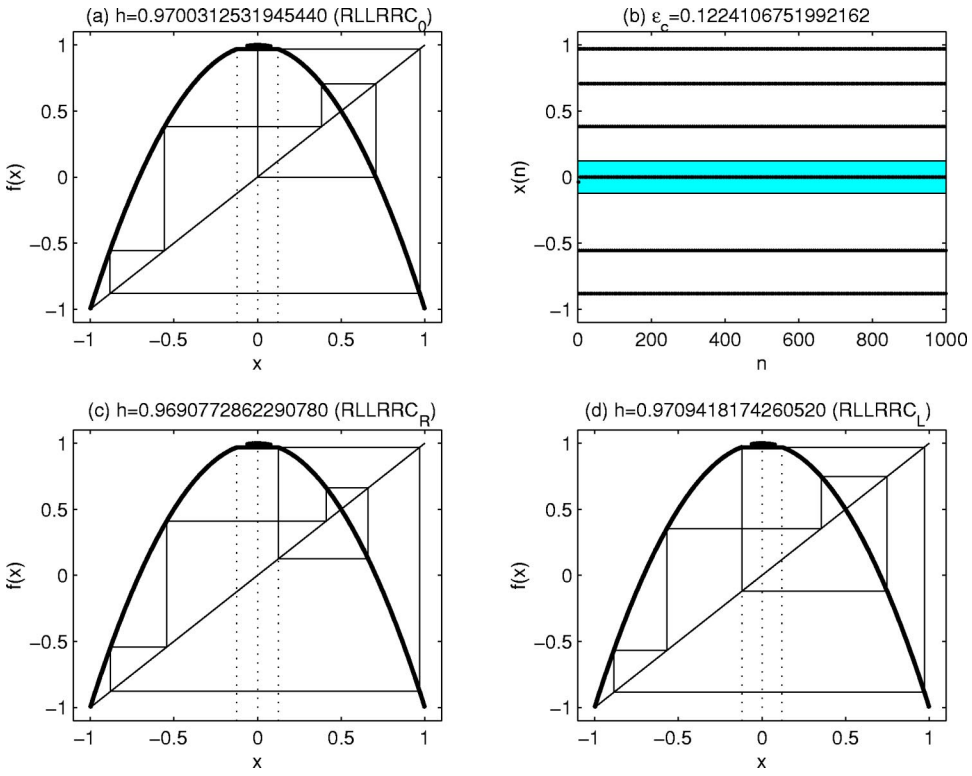

FIG. 4. Stabilization procedure of the target *RLLRR* using the limiter control (9). (a) Geometrical representation with $C_s=C_0$, (b) time series, (c) geometrical representation with $C_s=C_R$, and (d) geometrical representation with $C_s=C_L$.

$$B-\frac{1}{2}\cdot\underbrace{\frac{1}{2}\cdots}_{L}\left(\underbrace{B-\frac{1}{2}(\cdots x_0)}_{R}\right)=h, \tag{16}$$

where

$$x_0=\begin{cases} h/2 & \text{if } C_s=C_L, \\ B/2 & \text{if } C_s=C_0, \\ B-h/2 & \text{if } C_s=C_R. \end{cases} \tag{17}$$

For any admissible symbolic sequence of 1D unimodal maps, the relation between B and h can be obtained analytically from Eqs. (16) and (17). As an example, we again consider the period-5 UPO *RLLRR*. As shown earlier, such an orbit can be generated by using $RLLRRC_0$, $RLLRRC_R$, and $RLLRRC_L$, which yield $h=59B/64$, $58B/63$, and $12B/13$, respectively. We set $B=64$, 63, and 13, respectively. To minimize the configuration of the corresponding digital circuit [34] for any given target sequence, one should choose the smallest base B, or $13(<2^4-1)$. This choice of the optimal base means that a four-bit machine is sufficient to generate the binary sequence 10011 with $C_s=C_L$. For the other two cases, to generate such a sequence one must use seven-bit (for $B=64$) and six-bit (for $B=63$) machines.

In principle, the approach here can be used to stabilize an arbitrarily long periodic orbit with a computer of any precision. Figure 5 shows the control of a 508-period sequence, where the optimal parameters are $B=1019$, $h=1018$, and $C_s=C_R$. However, it should be pointed out that at present such a long sequence has not been successfully controlled using the logistic map with either the CF or limiter controller even when a 53-bit floating-point computer is used. In fact, bit error appears after about 50 cycles. To stabilize higher-period target sequences by the logistic map, a high-precision computer is needed.

D. Generation of *m* sequences by unimodal maps

We now turn our attention to *m* sequences. In particular, we consider whether the simplest chaotic map, the unimodal map, can be employed to generate any *m* sequence. We shall start with a brief introduction to the linear feedback shift register (LFSR). The LFSR is a typical finite-state machine and has been extensively studied and generalized to a far broader class of logical machines. The *m* sequence is derived from the class of irreducible polynomials [1]. Mathematically, a LFSR can be expressed as a "feedback function" $f(x)=\Sigma_{i=1}^{\oplus m}c_i x^i \oplus 1$, where the symbols $\oplus$ and $\Sigma^{\oplus}$ denote modulo-2 additions, and c_i, $x\in\{0,1\}$ are the feedback connections and states, respectively. With appropriate choice of the line feedback c in this function, one can obtain an *m* sequence. Its period is $L=2^m-1$, where m represents the number of stages of a LFSR. For example, using the line feedback $c=[10100]$ with initial state $x=[00001]$, as shown in Fig. 6(a), one gets a period-31 *m* sequence 1000010010110011111000110111010.

Surprisingly, this binary sequence corresponds to a SPO (also UPO) of the unimodal map [35]. For the CF control, the controlling parameter of the logistic map is given by $\gamma \approx -0.005\,827\,220\,839\,239$. For the limiter control, the parameter pair $[\epsilon_c,h]$ is approximately [0.043 770 157 829 400 2, 0.996 168 346 567 178 8], [0.043 770 157 819 215 6, 0.996 168 346 568 961 9], and [0.043 770 157 809 031 0, 0.996 168 346 570 745 0], for $\{C_L,C_0,C_R\}$, respectively. For the digital tent map, the parameter pair of the limiter control

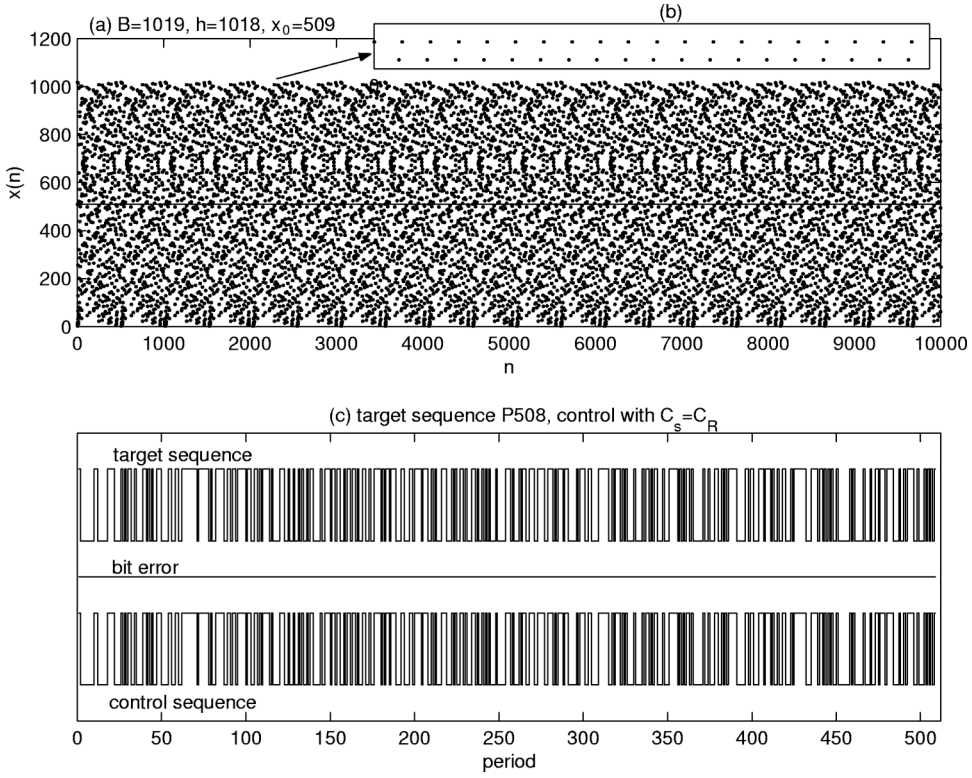

FIG. 5. A 509-period target sequence is generated by the digital tent map for $B=1019$, $h=1018$, and $C_s=C_R$. (a) Time series, (b) an enlargement of (a), and (c) binary representation. Note that the error of bit between the target sequence and the control sequence is zero.

can be given exactly by $[B,h]=[429\,496\,729\,5, 417\,525\,000\,8]$, [429 496 729 6, 417 525 000 9], and [429 496 729 7, 417 525 001 0], respectively. Figure 7 shows that this *m* sequence can be generated using the digital tent map with a 32-bit machine. Moreover, we find that by adding a state to the original LFSR, as shown in Fig. 6(b), its mirror sequence is easily formed. Examining this mirror sequence 10000011100100010101111101101001, we see that the sequence also corresponds to a period-32 SPO.

Table I gives the subset of all *m* sequences with $L=2^5-1$ and their corresponding mirror sequences. By examining these sequences [29], it is easily verified that these sequences are indeed admissible SPO sequences [36]. Their corresponding parameter values are given in Table I. Using these values, one can optimize the design of any new *m*-sequence generator based on chaotic hardware implementation [34].

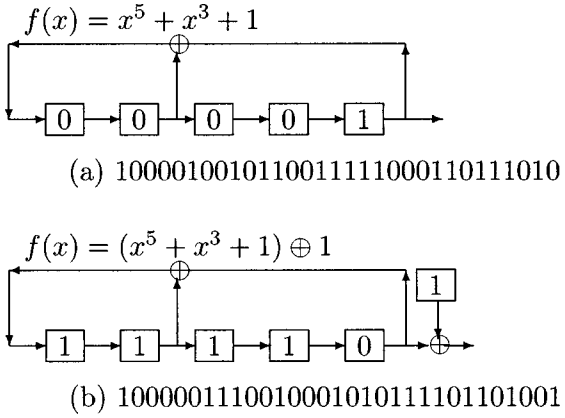

FIG. 6. (a) Five-stage shift register with line feedback connection $c=[10100]$; (b) its corresponding mirror sequence generator.

In principle, any unimodal map is capable of generating an arbitrarily long *m* sequence if we have an arbitrarily high-bit machine. To stabilize a period-*n* target sequence via the limiter controller one needs at least a 2^{2^n}-bit machine because of an anomalous superexponential scaling property, to be discussed in the next section. On the other hand, although the constant feedback control still obeys the well-known Feigenbaum scaling law in the control space, it cannot be used to generate very long periodic sequences robustly, since any rounding error of the shift iteration map can cause the calculated shift value (associated with a single superstable critical point) to go out of the accuracy range. How to handle this problem is a new challenge in chaos control.

IV. SCALING PROPERTIES

It is of practical interest to consider the convergence rate of the successive bifurcation points. If the bifurcation cascade is of any universality, it will be useful to find the strength required to convert a chaotic state to the desired stable states using one of the two control methods. To analyze the scaling behavior of the period-doubling bifurcation cascade in the control space, we calculate the rate of convergence of δ_n from the formula

$$\delta_n=\frac{\gamma_{n+1}-\gamma_n}{\gamma_{n+2}-\gamma_{n+1}}. \tag{18}$$

A. Constant feedback controller

For the CF method, the strength is determined by Eq. (8). Substituting Eq. (8) into Eq. (18) yields $\delta_n=(a_{n+1}^s$

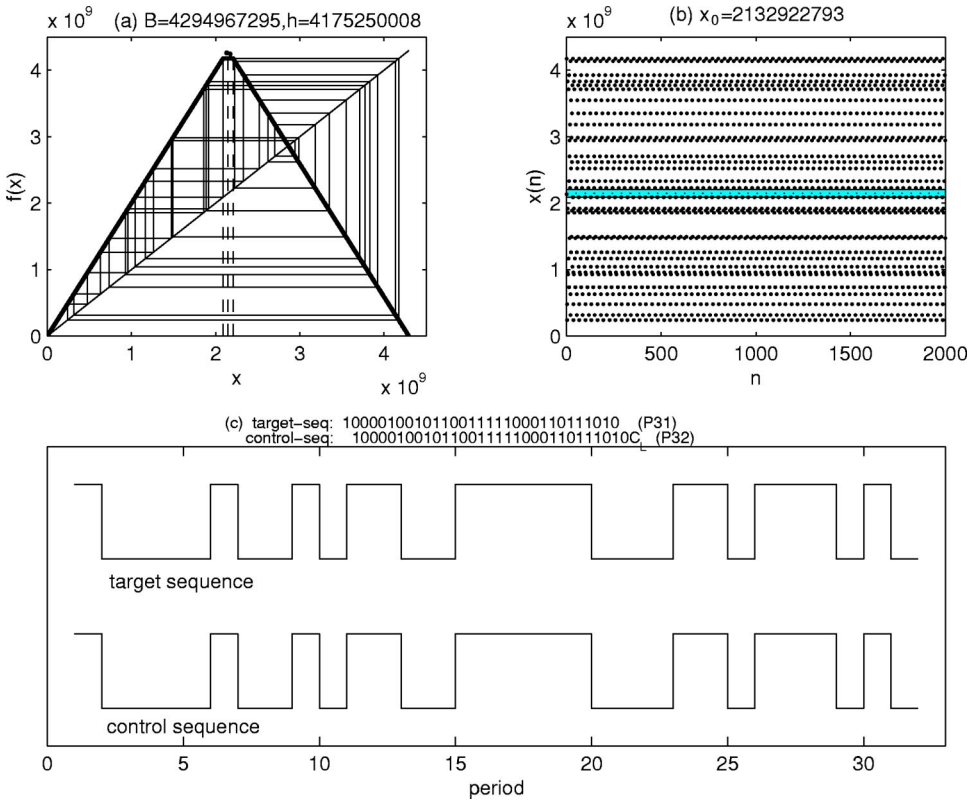

FIG. 7. Stabilization procedure of a period-31 maximum-length shift-register sequence using the digital tent map (14) with limiter control. (a) Geometrical representation, (b) time series, and (c) binary representation.

$-a_n^s)/(a_{n+2}^s-a_{n+1}^s)$ which is only related with superstable periodic points of the uncontrolled logistic map (for fixed system parameter a). Obviously, the iteration converges to $\gamma_n = \gamma_\infty - \text{const}/\delta^n$ with the Feigenbaum universal constant δ [31]. For the purpose of comparing with limiter control, we also estimate the parameter values corresponding to the 2^n ($n=1, \ldots, 12$) cycles by using the symbolic description. The result is shown in Table II. At our computer precision, γ_n converges to the Feigenbaum constant δ up to 4.669 201 and $\gamma_\infty \sim -0.299\,422$.

B. Limiter controller

Consider the scaling $\delta_n=(h_{n+1}-h_n)/(h_{n+2}-h_{n+1})$ of the limiter control. A superstable periodic orbit associated with different $C_s(=C_0, C_R, C_L)$ can give rise to different parameter values. As shown in Table III, the values of h_n corresponding to $C_s=C_0$ and $C_s\neq C_0$ for the period-doubling cascade are different. For both the logistic and tent maps, an infinite periodic sequence appears at $h_\infty \sim 0.852\,489\,223\,156\,092\,2$ and $h_\infty \sim 0.824\,908\,067\,280\,215\,2$, respectively. Beyond h_∞ chaos does not occur in the limiter control. Furthermore, it is seen

TABLE I. A list of all m sequences and their corresponding mirror set with $L=31$. The parameters $[B,h,C_s]$ correspond to the control values of the digital tent map discussed in Sec. IV C.

No.	connection	m sequence	$[B,h,C_s]$
1	10100	10000100101100111110001101110 10	[4294967295,4175250008,C_L]
2	10010	10000101011101100011111100110100	[4294967295,4188285872,C_L]
3	11110	10000101101010001110111111001001	[4294967295,4180718876,C_L]
4	11101	10000111001101111110100010010101	[1431655765,1398917956,C_L]
5	11011	10000110101001000101111110110011	[4294967295,4214778436,C_L]
6	10111	10000110010011111011100010101 10	[4294967295,4220178632,C_L]
		Mirror set of C_m sequence	
1	10100	10000011100100010101111101101001	[4294967295,4246629218,C_R]
2	10010	10000011001011011111010100010011	[1431655765,1419275966,C_R]
3	11110	10000011011001111101001010111000	[252645135,250404478,C_R]
4	11101	10000010111011010100111100011100	[1431655765,1413272058,C_R]
5	11011	10000010011000111110010101101110	[4294967295,4232219798,C_R]
6	10111	10000010001110101001011111001101	[1431655765,1410266886,C_R]

TABLE II. Controlling parameter and scaling coefficients of the feedback control (6) for the first few terms of the primary period-doubling bifurcation cascade $P=2^n$, $n=1,\ldots,12$, with $a=2$.

n	γ_n	δ_n
1	−0.5000000000000000	4.3856775985683534
2	−0.3446486793315834	4.6009492765380413
3	−0.3092262577839692	4.6551304953910275
4	−0.3015273201477196	4.6661119478267086
5	−0.2998734593926081	4.6685485814280785
6	−0.2995190185275788	4.6690606602814757
7	−0.2994430975301109	4.6691715545784955
8	−0.2994268370865245	4.6691951537908132
9	−0.2994233545750348	4.6692001793132869
10	−0.2994226087266872	4.6692011893566958
11	−0.2994224489887624	
12	−0.2994224147777874	

from Table III that these two maps with different C_s give almost the same superexponential relationship

$$\delta_n \sim 2^{2^n}+1, \quad n=0,\ldots,\infty. \tag{19}$$

As discussed, the parameter pair $[B,h]$ of the digital tent map can be analytically calculated. The parameter values corresponding to SPOs are listed in Table IV for the first few terms of the primary period-doubling bifurcation cascade. For $n\geqslant 0$, the parameters $[B_n,h_n]$ are given by

$$B_n=\begin{cases}2^{2^n} & \text{if } C_s=C_0,\\ 2^{2^n}+1 & \text{if } C_s\neq C_0,\end{cases} \tag{20}$$

$$h_n=B_n-\prod_{k=0}^{n-1}(2^{2^k}-1) \text{ for } n\geqslant 1, \tag{21}$$

and $h_0=1,2$ for $C_s=C_0$ and $C_s\neq C_0$, respectively. For $B=1$, we see that Eq. (21) reduces to Eq. (2) of Ref. [20] for $C_s\neq C_0$, and Eq. (10) of Ref. [33] for $C_s=C_0$, respectively.

For $C_s=C_0$, we get from Eqs. (20) and (21) and the definition of δ

$$\delta_n=\frac{1-\dfrac{2^{2^n}}{2^{2^n}-1}}{\dfrac{2^{2^{n+1}}-1}{2^{2^{n+1}}}-1}=\frac{2^{2^{n+1}}}{2^{2^n}-1}\approx 2^{2^n}+1, \tag{22}$$

which is consistent with the numerical results given in Table III and Eq. (19). The same scaling is also valid for $C_s\neq C_0$.

C. Sarkovskii sequences

To compare the scaling properties of the two controllers, we now consider the family of Sarkovskii sequences defined by $R^{*m}*(RLR^{2n})$ [29,37–39], where $n,m=0,1,\ldots$, and the symbol $*$ denotes an $*$-composition rule [40,41]. For $m=0,1,\ldots$, fixed $n=0$ gives the period-doubling bifurcation cascade. For $n\neq 0$, from the existence of a period-3 (RLC_s) it follows that the orbits must have all possible periods.

According to Eq. (8), it is clear that uncontrolled and controlled (with CF) logistic systems are of the same scaling

TABLE III. Controlling parameter and scaling coefficients of the limiter control for the first few terms of the primary period-doubling bifurcation cascade $P=2^n, n=0,\ldots,6$ for the logistic map (9), and the tent map (14) with $B=1$.

	$C_s=C_0$		$C_s\neq C_0$	
n	h_n	δ_n	h_n	δ_n
		Logistic map		
0	0	5.6858369565984210	0.5	7.5003867514630684
1	0.7071067811865476	6.2539199810038868	0.8090169943749475	18.203474114051435
2	0.8314696123025452	17.603429384436126	0.8502171357296141	257.91467840874850
3	0.8513551931052652	257.45753068379724	0.8524804477269028	65537.891229309535
4	0.8524848355384778	65537.497007586746	0.8524892231560922	
5	0.8524892232230416		0.8524892232899908	
6	0.8524892232899908			
		Tent map		
0	0.5	1.3333333333333339	0.6666666666666666	12.750000000000048
1	0.75	5.3333333333333330	0.8	17.133333333333333
2	0.8125	17.066666666666666	0.8235294117647058	257.00784313301438
3	0.82421875	257.00392156862745	0.8249027237354085	65537.070883511173
4	0.8249053955078125	65537.070867171031	0.8249080671986817	
5	0.8249080672394484		0.8249080672802152	
6	0.8249080672802152			

TABLE IV. Parameters corresponding to the period-doubling cascade ($P=2^n, n=0,\ldots,5$) of the digital tent map. Here, the column $[B,h]C_s$ indicates that a superstable periodic sequence is generated with the given parameters. For example, a period-4 SPO 101C can be implemented through $[B,h]=\{[16,13],[17,14]\}$, which correspond to $101C_0$ and $101C_R$, respectively.

n	Superstable sequence C	$[B,h]C_0$	$[B,h]C_s$	$B-h$
0		[2,1]	$[3,2]C_R$	1
1	1	[4,3]	$[5,4]C_L$	1
2	101	[16,13]	$[17,14]C_R$	3
3	1011101	[256,211]	$[257,212]C_L$	45
4	101110101011101	[65536,54061]	$[65537,54062]C_R$	11475
5	10111010101110111011010101101	[4294967296,3542953171]	$[4294967297,3542953172]C_L$	752014125

as Sarkovskii sequences. For the limiter control, these numerical results also suggest that a superexponential scaling $\delta_{h,m}\sim 2^{2^{m+1}}$ perhaps exists in the unimodal map. In order to verify this relation, we again consider the digital tent map (14). For $C_s=C_0$, the parameter values corresponding to some Sarkovskii sequences are listed in Table V. Obviously, the parameter B can be expressed in the form

$$B_{m,n}=[2^{2n+3}]2^m, \quad m,n=0,1,\ldots. \tag{23}$$

To obtain information on the height h, we note that $d=B-h$ satisfies

$$d_{m,n>0}=d_{m,n=0}+\begin{cases}\sum_{i=1}^{n}2^{2i},\\ \sum_{i=1}^{n}2^{4i-1}\times 3\times 7,\\ \sum_{i=1}^{n}2^{8i-3}\times 3^2\times 5\times 127\end{cases} \tag{24}$$

for $m=0,1,2$, respectively, and

$$d_{m,n=0}=\begin{cases}1 & \text{if } m=0,\\ 11 & \text{if } m=1,\\ 717 & \text{if } m=2.\end{cases} \tag{25}$$

Thus, the height h for $m\leqslant 2$ is $h_{m,n}=B_{m,n}-d_{m,n}$, and the rate of convergence is

$$\delta^B_{h,n}=\begin{cases}\dfrac{1}{4} & \text{if } m=0,\\ \dfrac{1-2^{2n}\times 7}{4-2^{2n+4}\times 7} & \text{if } m=1,\\ \dfrac{1-2^{6n+2}\times 7\times 5\times 127}{4-2^{6n+10}\times 3\times 5\times 127} & \text{if } m=2.\end{cases} \tag{26}$$

For $B=1$, Eq. (26) becomes

$$\delta_{h,m}=\lim_{n\to\infty}\frac{1}{\delta^B_{h,m,n}}=2^{2^{m+1}}, \quad m=0,1,2,\ldots. \tag{27}$$

The analytical and numerical results obtained here from the logistic and digital tent maps show that the Sarkovskii sequences in the limiter control of 1D unimodal maps indeed obey the superexponential scaling $\delta_{h,m}\sim 2^{2^{m+1}}$.

V. CONCLUSION AND DISCUSSION

In conclusion, we have investigated in detail the stabilization mechanism of arbitrary periodic orbits by applying symbolic dynamics to the feedback and limiter control schemes. We have shown that the strength of the feedback control is associated with the superstable parameters of the periodic orbits embedded in chaos, while the superstable plateau of the limiter control corresponds to the location of the unstable periodic orbits in the original chaotic system. It is found that the scaling behavior of the period-doubling bifurcation cascade for these two methods is completely different in the control space. In fact, the feedback control obeys the well-known Feigenbaum scaling law, while the limiter control exhibits anomalous superexponential scaling. Using symbolic dynamics, we have obtained analytically a more general scaling coefficient, corresponding to the sequence of period-doubling bifurcations of the controlled digital tent map. For the Sarkovskii sequence, we have also investigated the control parameter and obtained the scaling law. It is found that the strength of the feedback control obeys the same scaling relation as the superstable parameter of the original chaotic system. For the limiter control, a different superexponential relation quantitatively describing the fine structure of the Sarkovskii sequence is found. Furthermore, the control parameters, obtained exactly for the digital tent map, make sure that the periodic PN sequence generator based on chaos can be optimally configured.

To apply our control-parameter estimating technique to digital communications, we have as a simple example also investigated how to use 1D unimodal maps with limiter control to generate m sequences. Because the set of m sequences is only a subset of the SPOs (also UPOs) of 1D unimodal maps [36], an arbitrarily long m-sequence generator can in principle also be implemented by employing any 1D unimodal map with an arbitrary-precision machine. However, an important question still remains: are there simple control techniques for stabilizing an arbitrarily long UPO orbit with a *low-bit* computer? This question is especially relevant to low-cost digital circuit implementation. There are several possible strategies to deal with this problem. The first is to split a long UPO sequence into several short (admissible)

TABLE V. Parameters corresponding to periodic orbits associated with the Sarkovskii theorem. The length of the periodic sequences is $P=(2n+3)\times 2^m$, where $m,n=0, 1,\ldots$. The symbol—means that the corresponding sequence cannot be represented when a 53-bit computer is used.

m/n	6	5	4	3	2	1	0
			P				
2	60	52	44	36	28	20	12
1	30	26	22	18	14	10	6
0	15	13	11	9	7	5	3
			B				
2	—	4503599627370496	17592186044416	68719476736	268435456	1048576	4096
1	1073741824	67108864	4194304	262144	16384	1024	64
0	32768	8192	2048	512	128	32	8
			h				
2	—	3715055758791379	14511936557779	56687252179	221434579	864979	3379
1	885837005	55364813	3460301	216269	13517	845	53
0	27307	6827	1707	427	107	27	7
			$d=B-h$				
2	⋯—	788543868579117	3080249486637	12032224557	47000877	183597	717
1	187904819	11744051	734003	45875	2867	179	11
0	5461	1365	341	85	21	5	1

symbolic sequences. For this, the $*$-composition rule introduced in Sec. IV C can be a guide for the splitting. One can then optimize the resulting sequences with low-bit hardware using the direct and simple parameter-estimating procedure introduced here. However, for spread spectrum communications it may not be suitable with respect to miniaturization, power efficiency, high data rate, and high security. The second strategy is to develop new control techniques for extending the period length [42]. However, a problem with this approach is that the obtained sequences may not have the necessary randomness [1] and correlation [2,3] properties. The latter property is especially relevant to receiver synchronization as well as multiuser communication. The third, and more practical, strategy is to apply limiter control to high-speed chaotic analog oscillators, and design a symbolic synchronization receiver [17,18]. Our parameter-estimation technique can then be useful, such as in preparing the lookup table.

Although the use of UPO sequences in spread spectrum systems implies that the randomlike character of chaotic systems is partially lost, most of the long periodic sequences are in fact still very close to random sequences. Furthermore, for applications such as in direct spread spectrum communications, the corresponding security can be provided by other encryption techniques [3,43,44] involving chaos-based cryptography [45]. Such nonlinear encoding, while not critical for the present problem, should be of interest for future investigations.

[1] S. W. Golomb, *Shift Register Sequences* (Aegean Park, Laguna Hills, CA, 1982).

[2] R. C. Dixon, *Spread Spectrum Systems with Commercial Applications* (Wiley, New York, 1994).

[3] B. Sklar, *Digital Communications, Fundamentals and Applications* (Prentice-Hall, Upper Saddle River, NJ, 2001).

[4] See, for example, T. Kohda, and A. Tsuneda, in *Chaotic Electronics in Telecommunications*, edited by M. P. Kennedy, R. Rovatti, and G. Setti (CRC Press, Boca Raton, FL, 2000).

[5] L. Cong and X. F. Wu, IEEE Trans. Circuits Syst., I: Fundam. Theory Appl. **48**, 521 (2001).

[6] G. M. Maggio and N. Rulkov, IEEE Trans. Circuits Syst., I: Fundam. Theory Appl. **48**, 1424 (2001).

[7] D. S. Broomhead, J. P. Huke, and M. R. Muldoon, Dyn. Stab. Syst. **14**, 95 (1999).

[8] T. L. Carroll, IEEE Trans. Circuits Syst., I: Fundam. Theory Appl. **47**, 443 (2000).

[9] E. M. Bollt, T. Stanford, Y. C. Lai, and K. Życzkowski, Phys. Rev. Lett. **85**, 3524 (2000), and references therein.

[10] Z. Ben Jemaa and S. Belghith, in *11th International IEEE Workshop on Nonlinear Dynamics of Electronic Systems, Scuol, Switzerland, 2003*, edited by R. Stoop (IEEE, 2003), p. 303.

[11] See for example, S. Boccalett, C. Grebogi, Y. C. Lai, H. Mancini, and D. Maza, Phys. Rep. **329**, 103 (2000).

[12] E. R. Hunt, Phys. Rev. Lett. **67**, 1953 (1991).

[13] E. Ott, C. Grebogi, and J. A. Yorke, Phys. Rev. Lett. **64**, 1196 (1990).

[14] S. Parthasarathy and S. Sinha, Phys. Rev. E **51**, 6239 (1995).

[15] K. Myneni, T. A. Barr, N. Corron, and S. Pethel, Phys. Rev. Lett. **83**, 2175 (1999).

[16] N. Corron and S. Pethel, Chaos **12**, 1 (2002).

[17] N. Corron, S. Pethel, and K. Myneni, Phys. Rev. E **66**, 036204 (2002).
[18] S. Pethel, N. Corron, Q. R. Underwood, and K. Myneni, Phys. Rev. Lett. **90**, 254101 (2003).
[19] C. Wagner and R. Stoop, Phys. Rev. E **63**, 017201 (2000).
[20] R. Stoop and C. Wagner, Phys. Rev. Lett. **90**, 154101 (2003).
[21] S. Gueron, Phys. Rev. E **57**, 3645 (1998).
[22] J. Marín and R. V. Solé, Phys. Rev. E **65**, 026207 (2002).
[23] J. Güémez and M. A. Matías, Phys. Lett. A **181**, 29 (1993).
[24] C. Wieland, Phys. Rev. E **66**, 016205 (2002).
[25] N. Parekh and S. Sinha, Physica A **318**, 200 (2003).
[26] L. Yang, Z. R. Liu, and J. M. Mao, Phys. Rev. Lett. **84**, 67 (2000).
[27] G. Osipov, L. Glatz, and H. Troger, Chaos, Solitons Fractals **9**, 307 (1998).
[28] E. R. Weeks and J. M. Burgess, Phys. Rev. E **56**, 1531 (1997).
[29] B. L. Hao and W. M. Zheng, *Appllied Symbolic Dynamics and Chaos* (World Scientific, Singapore, 1998).
[30] H. Kaplan, Phys. Lett. **97A**, 365 (1983).
[31] M. Feigenbaum, J. Stat. Phys. **21**, 669 (1979).
[32] In all our examples, the two symbols C_L and C_R stand for C_L^b and C_R^b, which are associated with the left and right boundaries of the control window. With C_L and C_R given, one can calculate the maximum and minimum control values.
[33] P. H. Borcherds and G. P. McCauley, Chaos, Solitons Fractals **3**, 451 (1993).
[34] A. Dornbusch and J. P. de Gyvez, *Proceedings of the 1999 IEEE International Symposium on Circuits and Systems* (IEEE, 1999), Vol. 5, p. 454.
[35] N. Metropolis, M. L. Stein, and P. R. Stein, J. Comb. Theory, Ser. A **15**, 25 (1973).
[36] For the first time, it is computationally verified that the set of *m* sequences is a subset of the set of superstable periodic orbits of chaotic unimodal maps. A more detail paper is under preparation.
[37] T. Geisel and J. Nierwetberg, Phys. Rev. Lett. **47**, 875 (1981).
[38] S. J. Chang and J. McCown, Phys. Rev. A **31**, 3791 (1985).
[39] V. Urumov and L. Kocarev, Phys. Lett. A **144**, 220 (1990).
[40] T. Post and H. W. Capel, Physica A **178**, 62 (1991).
[41] B. Derrida, A. Gervois, and Y. Pomeau, J. Phys. A **12**, 269 (1979).
[42] J. Cernák, Phys. Lett. A **214**, 151 (1996).
[43] B. Schneier, *Applied Cryptography* (John Wiley, New York, 1996).
[44] J. Daemen and V. Dijmen, *The Design of Rijndael* (Springer, Berlin, 2002).
[45] L. Kocarev, IEEE Circuits Syst. Mag. **1**, 6 (2001).